

# Optimization Framework for the Analysis of Large-scale Networks of Energy Hubs

**Mads Almassalkhi**

malmassa@umich.edu  
 Department of Electrical Engineering and Computer Science  
 University of Michigan  
 Ann Arbor, USA

**Ian Hiskens**

hiskens@umich.edu

**Abstract** - Through a reformulation of energy hubs, this paper presents a novel format for describing general energy hub networks. This format underpins the development of tools for analyzing large-scale interconnected energy hub networks. The tools are developed in MATLAB and seamlessly interface with CPLEX optimization libraries to allow users to quickly implement and solve optimal scheduling problems. Our application takes a concise network description file as input, uses MATLAB to build the matrices for the entire system, and outputs the requested results from CPLEX. The work presented herein supports electrical and natural gas networks, wind generating capacity, district heat loads, and the main elements of energy hubs (converters and energy storage). Addition of other energy types and hub elements is straightforward.

**Keywords** - Energy hubs, coupled energy infrastructure, power system modeling, optimal energy flow.

## 1 Introduction

RECENT events have placed a renewed focus on the reliability and optimality of energy supply systems [1]. Such systems involve interconnections between the electrical network and various energy carriers, such as natural gas and wind energy. Energy hub concepts provide a framework for extending beyond specific energy carrier combinations, such as hydrothermal systems [2], allowing analysis and optimal scheduling of an arbitrary array of energy carriers. Coupling energy carriers may reveal minimum cost solutions, and also vulnerabilities, that are not apparent when each energy system is treated separately [3]. This paper therefore considers energy hub models that are suited to large-scale coupled energy systems.

Energy hubs represent a relatively new and general concept, which explicitly models couplings between different energy systems [4]. However, implementing even a small network of interconnected energy hubs has proven rather tedious due to the coding effort needed to set up the energy hub system. Furthermore, once a system is implemented, making relatively small changes to the network topology can involve time-consuming revisions of the code. In fact, there is a genuine need for developing tools that implement and simulate large-scale coupled energy systems [5]. The best tools currently available for simulating energy-hub systems focus on small-scale networks where a drag-and-drop interface allows users to manually construct energy-hub networks using blocks and connector lines [6]. Through a reformulation of the en-

ergy hub model, we can take advantage of its structure to construct a novel format that describes general large-scale energy hub systems and allows for simple implementation and analysis of multi-energy systems.

Our paper is organized as follows. In Section 2, we formulate the modified energy hub and network models. In Section 3, we discuss our ASCII energy-hub format. That format is employed in Section 4 to simulate a large energy hub network. Section 5 presents concluding remarks and future work.

## 2 Model

There are many ways to formulate multi-carrier energy networks. We will focus our discussion on the “hybrid energy hub” model developed in [7, 8]. Table 1 categorizes the variables that arise in the model and are described in detail in the following subsections. The decision variables are those quantities that a system controller could directly manipulate. In our model, we control converter, generator, and energy storage utilization.

Variable Type	Variables
Decision	$\hat{\mathbf{P}}, \mathbf{f}_G, \mathbf{Q}$
Dependent	$\mathbf{P}, \mathbf{L}, \mathbf{f}, \mathbf{f}_D, \mathbf{E}, \hat{\mathbf{E}}, \mathbf{z}, \mathbf{\Gamma}, \mathbf{\Lambda}$
Constant Parameter	$\mathbf{S}_{in,out}, \mathbf{F}, \mathbf{C}, \eta_{ch}, \eta_{dis}$

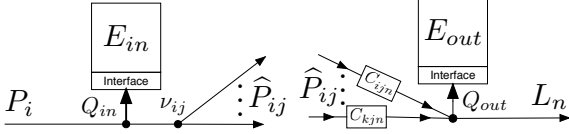
**Table 1:** Variables that arise in the energy hub model.

### 2.1 Energy Hub Model

Most common energy hubs can be constructed from interconnections of five simple building blocks: input sources, input storage, converters, output storage, and output sources. In describing the flow of power from hub input to hub output, we need to consider the flow between each of the five blocks of the hub. Let  $h \in \mathcal{H}$  be a hub from the set of available hubs, where  $h$  has input sources  $i \in \{1, 2, \dots, N_{in}\}$  and output sources  $n \in \{1, 2, \dots, N_{out}\}$ . Let  $P_i$  be the input flow from source  $i$  at hub  $h$ . Referring to Figure 1(a), to describe the flow from input source  $i$  to a converter  $j$ , we have to take into account any input storage devices and possible dispatch factors. The dispatch factors  $\nu_{ij} \in [0, 1]$  determine the dispatch flows  $\hat{P}_{ij}$ , which describe the amount of input flow  $i$  that is directed to converter  $j$ .

From Figure 1(a), we see that

$$P_i = Q_i^{in} + \sum_{j=1}^{k_i} \hat{P}_{ij} \quad (1)$$



(a) From input to converters. (b) From converters to output.

**Figure 1:** Decomposing the energy hub model based on dispatch flows.

where  $Q_i^{in}$  is the flow going into input storage device  $i$  and  $\hat{P}_{ij}$  is one of the  $k_i$  flows determined by the dispatch factors,  $\nu_{ij}$ , such that

$$\hat{P}_{ij} = \nu_{ij}(P_i - Q_i^{in}) \quad (2)$$

and

$$\sum_{j=1}^{k_i} \nu_{ij} = 1, \quad 0 \leq \nu_{ij} \leq 1. \quad (3)$$

Note that (3) ensures conservation of flow between input storage and converter blocks. Employing (2) and (3), we can eliminate dispatch factors  $\nu_{ij}$  to obtain

$$0 \leq \hat{P}_{ij} \leq P_i - Q_i^{in}. \quad (4)$$

From (1) and (4), the relationship between input sources and input storage can be written in matrix form as,

$$\mathbf{P}_h = \mathbf{S}_h^{in} \mathbf{Q}_h^{in} + \mathbf{F}_h \hat{\mathbf{P}}_h \quad \forall h \in \mathcal{H} \quad (5)$$

$$\mathbf{0} \leq \hat{\mathbf{P}}_h \leq \mathbf{F}_h^\top \mathbf{P}_h - \mathbf{F}_h \mathbf{S}_h^{in} \mathbf{Q}_h^{in} \quad \forall h \in \mathcal{H} \quad (6)$$

where  $\mathbf{S}_h^{in}$  is the *input storage coupling matrix* and  $\mathbf{F}_h$  is the *dispatch flow matrix*.

Referring to Figure 1(b), output flows  $L_n$  are obtained by converting dispatch flows  $\hat{P}_{ij}$ . Converter  $C_{ijn}$  converts the  $j$ -th dispatch flow of input source  $i$  into output source  $n$ . The output flows  $L_n$  must also take into account any output storage device flow,  $Q_n^{out}$ . Thus, modeling hub output flows gives,

$$\sum_i \sum_{j \in \mathcal{D}(i,n)} C_{ijn} \hat{P}_{ij} = Q_n^{out} + L_n. \quad (7)$$

where  $\mathcal{D}(i, n)$  is the set of dispatch flows from input  $i$  that can be converted to output  $n$ , and  $|\mathcal{D}(i, n)| \leq k_i$ .

From (7), we can rewrite the output flows for hub  $h$  in matrix form,

$$\mathbf{L}_h = \mathbf{C}_h \hat{\mathbf{P}}_h + \mathbf{S}_h^{out} \mathbf{Q}_h^{out} \quad \forall h \in \mathcal{H} \quad (8)$$

where  $\mathbf{C}_h$  is the *converter coupling matrix* and  $\mathbf{S}_h^{out}$  is the *output storage coupling matrix*.

With regard to input and output energy storage devices, we must consider multiple time periods since energy source  $p$ , stored at time  $t \in \{1, 2, \dots, T\}$ , depends on the power available in the previous time step. If we assume steady-state storage power values, a constant slope for  $\dot{E}_p = dE_p/dt$ , and treat storage interface as a converter device with charging and discharging efficiencies  $\eta_{ch}$  and  $\eta_{dis}$ , the relationship between storage flows  $Q$  and the change in energy levels is,

$$\dot{E}_p = \frac{dE_p}{dt} \approx e_p Q_p \quad (9)$$

where

$$e_p = \begin{cases} \eta_{ch}, & \text{if } Q_p \geq 0 \quad (\text{charge/standby}) \\ 1/\eta_{dis}, & \text{if } Q_p < 0 \quad (\text{discharge}) \end{cases} \quad (10)$$

which yields for the energy storage level,

$$E_p^t = E_p^{t-1} + \dot{E}_p^t. \quad (11)$$

Since a storage device has two distinct states of operation, charging and discharging, that achieve different efficiencies, energy storage devices introduce switches in the energy hub formulation. To avoid this nonlinearity, we make use of binary variables to distinguish between the two states. Let the steady-state storage power flow be defined by the sum of a positive (charging) and a negative (discharging) power flow, such that

$$Q_p = Q_{p,ch} + Q_{p,dis} \quad (12)$$

with

$$-(1 - z_p) \underline{Q}_p \leq Q_{p,dis} \leq 0 \quad (13)$$

$$0 \leq Q_{p,ch} \leq z_p \bar{Q}_p \quad (14)$$

where  $z_p \in \{0, 1\}$ , and  $\bar{Q}_p$  and  $\underline{Q}_p$  are limits on the flow into and out of device  $p$ . Thus, when  $z_p = 0$ , storage device  $p$  is in discharging mode (as  $Q_{p,ch} \equiv 0$ ), while  $z_p = 1$  implies  $p$  is in charging mode (with  $Q_{p,dis} \equiv 0$ ). We can now write  $\dot{E}_p$  in terms of  $Q_{p,ch}$  and  $Q_{p,dis}$  as,

$$\dot{E}_p = \eta_{ch} Q_{p,ch} + \frac{1}{\eta_{dis}} Q_{p,dis}. \quad (15)$$

Notice that (9) is nonlinear because it involves the product of two state variables,  $e_p$  and  $Q_p$ . Equation (15) is an equivalent linear description. Therefore, by introducing additional binary variables  $z_p$ , we have removed a nonlinearity. We can now rewrite (11) in terms of the charging and discharging variables, giving

$$E_p^t = E_p^{t-1} + \eta_{ch} Q_{p,ch}^t + \frac{1}{\eta_{dis}} Q_{p,dis}^t. \quad (16)$$

The main difference between our linear formulation of energy hub flows in equations (5) and (8), and the common input-to-output hub equation developed in [9],

$$\mathbf{L}_h = \mathbf{C}_h \mathbf{P}_h - \mathbf{S}_h \mathbf{Q}_h, \quad (17)$$

is that we explicitly take into account the dispatch factor flows, and our four matrices  $\mathbf{S}_h^{in}$ ,  $\mathbf{F}_h$ ,  $\mathbf{C}_h$ , and  $\mathbf{S}_h^{out}$  are all constant. In the case of (17), the matrices  $\mathbf{C}_h$  and  $\mathbf{S}_h$  depend on the dispatch factor control variables  $\nu_{ij}$ , which introduce a nonlinearity. Thus, along with our reformulation of energy storage via binary variables, we have constructed a strictly linear description for hub  $h$ .

Furthermore, since each hub  $h$  is completely described by its local matrices  $\mathbf{S}_h^{in}$ ,  $\mathbf{F}_h$ ,  $\mathbf{C}_h$ , and  $\mathbf{S}_h^{out}$ , each hub is

decoupled and we can describe the entire set of hubs  $\mathcal{H}$  by constructing block-matrices from the  $h$ -specific matrices. For example, the converter coupling matrix for  $\mathcal{H}$  is defined as:

$$\mathbf{C} = \begin{pmatrix} \mathbf{C}_1 & 0 & \cdots & 0 \\ 0 & \mathbf{C}_2 & \ddots & \vdots \\ \vdots & \ddots & \ddots & 0 \\ 0 & \cdots & 0 & \mathbf{C}_{|\mathcal{H}|} \end{pmatrix}.$$

Thus, we can describe  $\mathcal{H}$  for all  $t$  by the mixed-integer linear relations,

$$\mathbf{0} \leq \widehat{\mathbf{P}}^t \leq \mathbf{F}^\top \mathbf{P}^t - \mathbf{F}^\top \mathbf{S}_{in} \mathbf{Q}_{in}^t \quad (18)$$

$$\mathbf{P}^t = \mathbf{S}_{in} \mathbf{Q}_{in}^t + \widehat{\mathbf{P}}^t \quad (19)$$

$$\mathbf{L}^t = \mathbf{C} \widehat{\mathbf{P}}^t + \mathbf{S}_{out} \mathbf{Q}_{out}^t \quad (20)$$

$$\mathbf{E}_{in,out}^t = \mathbf{E}_{in,out}^{t-1} + \dot{\mathbf{E}}_{in,out}^t \quad (21)$$

$$\mathbf{Q}_{in,out}^t = \mathbf{Q}_{in,out,ch}^t + \mathbf{Q}_{in,out,dis}^t \quad (22)$$

$$\dot{\mathbf{E}}_{in,out}^t = \eta_{ch} \mathbf{Q}_{in,out,ch}^t + \frac{1}{\eta_{dis}} \mathbf{Q}_{in,out,dis}^t \quad (23)$$

$$-(1 - \mathbf{z}_{in,out}^t) \underline{\mathbf{Q}}_{in,out} \leq \mathbf{Q}_{in,out,dis}^t \leq \mathbf{0} \quad (24)$$

$$\mathbf{0} \leq \mathbf{Q}_{in,out,ch}^t \leq \mathbf{z}_{in,out}^t \overline{\mathbf{Q}}_{in,out} \quad (25)$$

$$z_{in,out} \in \{0, 1\}. \quad (26)$$

The formulation is mixed integer because the elements of  $\mathbf{z}$  are binary variables.

## 2.2 Interconnection of Energy Hubs

Energy hubs are interconnected via various energy supply networks. In the previous section, we defined how power flowed through an energy hub from input to output. To describe the flow of power between hubs, we need to include power networks. A power network is a simple graph with additional physical constraints corresponding to the specific nature of the network, e.g. electrical or natural gas. Let  $\mathcal{G} = (\mathcal{N}, \mathcal{A})$  be a simple graph with nodes  $\mathcal{N} = \{1, 2, \dots, N\}$  and arcs  $\mathcal{A} = \{1, 2, \dots, E\}$ . Define the sets of generator and load nodes as  $\mathcal{C}, \mathcal{D} \subset \mathcal{N}$  where generator nodes inject power into the network while load nodes consume power from the network. The remaining nodes are called throughput nodes and neither inject nor consume power. Every graph must satisfy flow balance. That is, the sum of flows into and out of node  $i$  must equal the flow injected  $G_i$ , or consumed  $-D_i$ , at node  $i$ . Thus, for each node  $i$  of each network we have,

$$\sum_{j \in \mathcal{C}(i)} f_{ij} = b_i = \begin{cases} G_i & i \in \mathcal{C} \\ -D_i & i \in \mathcal{D} \\ 0 & \text{otherwise} \end{cases} \quad (27)$$

where  $\mathcal{C}(i)$  is the set of nodes connected to node  $i$ , and  $f_{ij}$  is positive (negative) for flow out of (into) node  $i$ . In matrix form, this becomes,

$$\mathbf{A} \mathbf{f} = \mathbf{b} \quad (28)$$

where  $\mathbf{A} \in \mathbb{R}^{N \times E}$  is the sparse *node-arc incidence matrix* defined by,

$$\mathbf{A}(i, k) = \begin{cases} 1, & \text{if arc } k \text{ starts at node } i \\ -1, & \text{if arc } k \text{ ends at node } i \\ 0, & \text{otherwise.} \end{cases} \quad (29)$$

With the inclusion of energy hubs, we need to consider flows between energy hubs and networks, and (27) becomes,

$$\sum_{j \in \mathcal{C}(i)} f_{ij} = b_i - \sum_{l \in \mathcal{H}(i)} P_l + \sum_{m \in \mathcal{H}(i)} L_m \quad (30)$$

where  $\mathcal{H}(i)$  is the set of hubs connected to node  $i$ ,  $P_l$  is the power input to hub  $l$ , and  $L_m$  is the power output from hub  $m$ . As before,  $b_i$  contains generator and demand variables and can be separated into injected generator flows  $\mathbf{f}_G$  and consumed load flows  $\mathbf{f}_D$ . Thus, we can generalize the flow balance equation (28) to that of an interconnected system of energy hubs,

$$\mathbf{A} \mathbf{f} + \mathbf{H}_I \mathbf{P} + \mathbf{H}_O \mathbf{L} + \mathbf{G}_A \mathbf{f}_G + \mathbf{D}_A \mathbf{f}_D = \mathbf{0} \quad (31)$$

where  $\mathbf{P}$  is the vector of all hub inputs,  $\mathbf{L}$  is the vector of all hub outputs,  $\mathbf{f}_G$  is the vector of all generator flows,  $\mathbf{f}_D$  is the vector of all load flows,  $\mathbf{H}_I$  is the hub input flow matrix,  $\mathbf{H}_O$  is the hub output flow matrix,  $\mathbf{G}_A$  is the generator-node matrix, and  $\mathbf{D}_A$  is the load-node matrix. For example, if hub input  $P_l$  is connected to node  $i$  then  $\mathbf{H}_I(i, l) = 1$ , and if generator  $f_{Gk}$  is at node  $i$  then  $\mathbf{G}_A(i, k) = -1$ . Otherwise the entries are all zeros. The other two matrices are defined in a similar manner. Since we assume the network topology does not change between time steps, the matrices are constant. Thus, we can restate (31) as,

$$\Lambda_n(\mathbf{f}, \mathbf{f}_G, \mathbf{f}_D, \mathbf{P}, \mathbf{L}) = \mathbf{0} \quad (32)$$

where  $n \in \mathcal{N}$  refers to the network type. Thus, the coupling between energy hubs and power networks only takes place at hub inputs and outputs.

Besides being connected to energy hubs, the main difference between a graph and a power network lies in additional constraints arising from the specific energy type of a network. For example, the added constraints imposed on an electrical power network often come in the form of the linear DC flow model,

$$f_{ij} x_{ij} - (\theta_i - \theta_j) = 0 \quad (33)$$

where  $x_{ij}$  is the reactance of arc  $(i, j)$  and  $\theta_i$  is the phase angle at node  $i$  [2]. This model approximates the nonlinear AC power flow<sup>1</sup>. Other physical constraints are also often nonlinear. A common nonlinear physical constraint is seen with natural gas networks, where the power flow through pipelines depends in a nonlinear manner on the pressure,  $p_i$ , applied at the nodes [10],

$$f_{ij} = \begin{cases} k_{ij} \sqrt{p_i - p_j} & \text{if } p_i \geq p_j \\ -k_{ij} \sqrt{p_j - p_i} & \text{if } p_i < p_j \end{cases} \quad (34)$$

<sup>1</sup>We recognize the limitations of the approximate DC flow model, however, we are primarily concerned with energy exchanges between the multiple networks, and in that context, this approximate model is sufficient.

where  $k_{ij}$  is a constant pertaining to the specific gas and pipeline properties. In addition, power is necessary to maintain pressure at the nodes, which introduces the compressor constraints,

$$f_{com,ij} = k_{com} f_{ij} (p_i - p_j) \quad (35)$$

with  $k_{com}$  a constant describing the properties of the compressor. In general, however, we will denote the physical constraints of any network  $n$  by an equation of the form,

$$\Gamma_n(\mathbf{f}, \xi_n, \mathbf{A}_n) = 0 \quad (36)$$

where  $\xi_n$  are the state variables associated with the physical constraints, and  $\mathbf{A}_n$  is the node-arc incidence matrix for network  $n$ . Note that  $\Gamma_n$  is independent of the energy hubs.

### 2.3 Optimal Power Dispatch Formulation

Our optimal power dispatch formulation is similar to that found in [8], and is given by,

$$\min_{\hat{\mathbf{P}}, \mathbf{f}_G, \mathbf{Q}} \sum_{t=1}^{N_T} \mathcal{F}^t(\mathbf{P}^t, \hat{\mathbf{P}}^t, \mathbf{L}^t, \mathbf{f}_G^t, \mathbf{f}_D^t) \quad (37a)$$

subject to

$$\mathbf{P}^t = \mathbf{S}_{in} \mathbf{Q}_{in}^t + \mathbf{F} \hat{\mathbf{P}}^t \quad \forall t \quad (37b)$$

$$\mathbf{L}^t = \mathbf{C} \hat{\mathbf{P}}^t + \mathbf{S}_{out} \mathbf{Q}_{out}^t \quad \forall t \quad (37c)$$

$$\mathbf{Q}_{in}^t = \mathbf{Q}_{in,ch}^t + \mathbf{Q}_{in,dis}^t \quad \forall t \quad (37d)$$

$$\mathbf{E}_{in}^t = \mathbf{E}_{in}^{t-1} + \dot{\mathbf{E}}_{in}^t \quad \forall t \quad (37e)$$

$$\dot{\mathbf{E}}_{in}^t = \eta_{ch}^{in} \mathbf{Q}_{in,ch}^t + \frac{1}{\eta_{dis}^{in}} \mathbf{Q}_{in,dis}^t \quad \forall t \quad (37f)$$

$$\mathbf{Q}_{out}^t = \mathbf{Q}_{out,ch}^t + \mathbf{Q}_{out,dis}^t \quad \forall t \quad (37g)$$

$$\mathbf{E}_{out}^t = \mathbf{E}_{out}^{t-1} + \dot{\mathbf{E}}_{out}^t \quad \forall t \quad (37h)$$

$$\dot{\mathbf{E}}_{out}^t = \eta_{ch} \mathbf{Q}_{out,ch}^t + \frac{1}{\eta_{dis}} \mathbf{Q}_{out,dis}^t \quad \forall t \quad (37i)$$

$$\mathbf{0} \leq \hat{\mathbf{P}}^t \leq \mathbf{F}^\top \mathbf{P}^t - \mathbf{F}^\top \mathbf{S}_{in} \mathbf{Q}_{in}^t \quad \forall t \quad (37j)$$

$$\mathbf{0} \leq \mathbf{E}_{in}^t \leq \mathbf{E}_{in}^{\max} \quad \forall t \quad (37k)$$

$$(\mathbf{1} - \mathbf{z}_{in}^t) \mathbf{Q}_{in}^t \leq \mathbf{Q}_{in,dis}^t \leq \mathbf{0} \quad \forall t \quad (37l)$$

$$\mathbf{0} \leq \mathbf{Q}_{in,ch}^t \leq \mathbf{z}_{in}^t \bar{\mathbf{Q}}_{in} \quad \forall t \quad (37m)$$

$$\mathbf{0} \leq \mathbf{E}_{out}^t \leq \mathbf{E}_{out}^{\max} \quad \forall t \quad (37n)$$

$$(\mathbf{1} - \mathbf{z}_{out}^t) \mathbf{Q}_{out}^t \leq \mathbf{Q}_{out,dis}^t \leq \mathbf{0} \quad \forall t \quad (37o)$$

$$\mathbf{0} \leq \mathbf{Q}_{out,ch}^t \leq \mathbf{z}_{out}^t \bar{\mathbf{Q}}_{out} \quad \forall t \quad (37p)$$

$$\mathbf{z}_{in}^t, \mathbf{z}_{out}^t \in \{0, 1\} \quad \forall t \quad (37q)$$

$$\hat{\mathbf{P}}^{\min} \leq \hat{\mathbf{P}}^t \leq \hat{\mathbf{P}}^{\max} \quad \forall t \quad (37r)$$

$$\hat{\mathbf{L}}^{\min} \leq \hat{\mathbf{L}}^t \leq \hat{\mathbf{L}}^{\max} \quad \forall t \quad (37s)$$

$$\Lambda_n(\mathbf{f}^t, \mathbf{f}_G^t, \mathbf{f}_D^t, \mathbf{P}^t, \mathbf{L}^t) = \mathbf{0} \quad \forall n, \forall t \quad (37t)$$

$$\Gamma_n(\mathbf{f}^t, \xi_n^t, \mathbf{A}_n) = \mathbf{0} \quad \forall n, \forall t \quad (37u)$$

$$\mathbf{f}_G^{\min} \leq \mathbf{f}_G^t \leq \mathbf{f}_G^{\max} \quad \forall t \quad (37v)$$

$$\mathbf{0} \leq |\mathbf{f}_G^t - \mathbf{f}_G^{t-1}| \leq \bar{\mathbf{f}}_G^{\max} \quad \forall t \quad (37w)$$

$$\mathbf{f}_D^{\min} \leq \mathbf{f}_D^t \leq \mathbf{f}_D^{\max} \quad \forall t \quad (37x)$$

$$\mathbf{f}^{\min} \leq \mathbf{f}^t \leq \mathbf{f}^{\max} \quad \forall t \quad (37y)$$

where  $t \in \{1, 2, \dots, T\}$  and  $n \in \mathcal{N}$ .

We are interested in studying optimal dispatch of power across interconnected energy hub systems under various conditions, with the aim of determining how best to employ energy hubs, energy hub storage, network generators, and energy sources. We see from (11) and (23) that energy storage devices require optimization over multiple periods with binary variables. In addition, the physical constraints in (36) are often nonlinear, which means our formulation is a *multi-period nonlinear mixed-integer programming problem*.

The objective function in (37a) may take a variety of forms for different studies. It will, therefore, depend on a range of variables, including energy hub inputs, outputs, and converter utilization, as well as network loads and generators. Equality constraints (37b)-(37i) describe the energy hub flow equations from Section 2.1, while inequality constraints (37j)-(37s) pertain to limits on dispatch flows, energy storage levels, charge/discharge flows, and hub input and output flows. The flow balance and physical constraints from Section 2.2 are described by equality constraints (37t)-(37u). Finally, the inequality constraints (37v)-(37y) arise from limits on network generators and loads, and flow capacities of network arcs.

## 3 Automated Analysis

We employ the energy hub network formulation presented in the previous section to develop a concise ASCII-based format for describing a general energy hub network. Such a format allows us to take advantage of the inherent flexibility of the energy hub model and easily interface with MATLAB.

### 3.1 Header Information

Before establishing the energy hub and network formats, we need to initialize the system with a system header that describes how many hubs and networks the system employs. The header also allows users to specify the number of time-intervals they desire for the optimal dispatch problem.

### 3.2 Hub Format

To characterize a general energy hub, we only need to know the four matrices:  $\mathbf{S}_h^{in}$ ,  $\mathbf{F}_h$ ,  $\mathbf{C}_h$ , and  $\mathbf{S}_h^{out}$  from (5), (6), and (8). In order to construct these four matrices, we need to take advantage of the simple building blocks that make up any energy hub and the knowledge that the flow of any hub input must enter input storage ( $\mathbf{S}_h^{in}$ ), divide into dispatch flows ( $\mathbf{F}_h$ ), enter converters ( $\mathbf{C}_h$ ), and/or enter output storage ( $\mathbf{S}_h^{out}$ ) before reaching a hub output. Therefore, by describing each hub's input flow to a converter, possibly through an input storage device and dispatch factors, and from converter to output, possibly through an output storage device, we can construct the four matrices that characterize that specific energy hub. This hub description can be captured by our ASCII-format description file.

An example energy hub is shown in Figure 2 with accompanying ASCII-format description in Listing 1. The

first line of Listing 1 (starting with “H”) identifies the hub ID number (1), the number of hub dispatch factors (3), the number of hub inputs (2), and the number of hub outputs (2). Next, the format describes how the power flows through the hub. Input 1 ( $P_1$ ) enters from node 3 in network 1, (1, 3), and has two dispatch factors that each enter a separate converter. The first dispatch factor,  $\text{df}(1, 2)$ , enters converter  $C^F$ , which has one output with efficiency 0.6,  $c(1, 0.6)$ . The output flow from this converter leaves the hub at  $L_1$  and is injected into node 1 of network 3, (3, 1). Line 2 represents the second dispatch factor  $\text{df}(2, 2)$  and is similar to line 1, except now we have two outputs from converter  $C^{CHP}$  into two different networks. The last line in Listing 1 represents input  $P_2$ . This input utilizes input storage  $E_{in}$  with charge and discharge efficiencies 0.8 and 0.7, respectively, initial storage level 0 p.u., and maximum energy storage capacity of 6 p.u.,  $s(0.8, 0.7, 0, 6)$ . With only one dispatch flow  $\hat{P}_{21}$ , described by  $\text{df}(1, 1)$ , the flow enters converter  $C^{TR}$ , which has one output with efficiency 0.8,  $c(1, 0.8)$ . Finally, the flow is injected into node 1 of network 2, (2, 1).

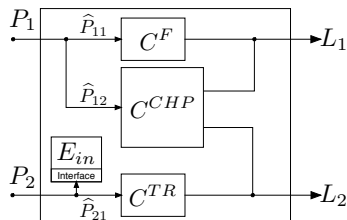


Figure 2: Example energy hub used to describe ASCII format.

```
H 1 3 2 2
(1,3) df(1,2) c(1,0.6) (3,1)
(1,3) df(2,2) c(2,0.3,0.35) (3,1) (2,1)
(2,5) s(0.8,0.7,0,6) df(1,1) c(1,0.8) (2,1)
```

Listing 1: Description of the energy hub in Figure 2.

To indicate output storage rather than input storage, the storage block  $s(0.8, 0.7, 0, 6)$  would be moved between the converter and output. In the case of multiple output converters, additional output storage flags can be used to denote which outputs employ output storage devices.

### 3.3 Network Format

To fully describe the networks that interconnect energy hubs, we need to consider (31) and (36). The matrices  $\mathbf{H}_I$  and  $\mathbf{H}_O$  from (31) can be constructed from the energy hub description of inputs and outputs in Section 3.2. Thus, for any network  $n$ , we only need to describe matrices  $\mathbf{A}$ ,  $\mathbf{G}_A$  and  $\mathbf{D}_A$  from (31) and  $\mathbf{\Gamma}_n$  from (36). To describe the first three matrices is relatively straightforward, as we just need to know how nodes of network  $n$  are connected and which nodes are generators and loads. However, describing  $\mathbf{\Gamma}_n$  is more difficult due to the potentially large variety of nonlinear physical networks and network parameters. For example, electricity, natural gas, and district heating are all different networks that require different physical constraints and parameters. Electrical networks (DC model) require reactance values, while natural

gas networks require pipeline length and diameter, operating temperatures and pressures, and gas-specific values to describe flows between nodes. Nonetheless, by assigning network types to each network and making simplifying assumptions about each network, it is possible to define network-specific formats that allow us to represent a simplified version of any network. For example, referring to (34), only a single parameter  $k_{ij}$  is required to describe the nonlinear flow of natural gas. Currently, our format supports the following networks: electrical DC model, linearized natural gas model with compressor stations, simplified district heating, and wind generators.

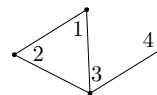


Figure 3: Example of a small electrical network (with nodal numbering).

```
IC 1 2 4 4 1 1 0
1 2 0.05 10
1 3 0.05 10
2 3 0.05 10
3 4 0.05 10

Generators
1 lim(0,100) (9,0.09)
Loads
3 lim(1)
```

Listing 2: Format for describing the network in Figure 3.

Figure 3 presents a simple electrical network (DC model), which is described by the network format in Listing 2. The first line (starting with IC) describes the network ID (1), network type (2), number of nodes (4), number of arcs (4), number of generators (1), number of loads (1), and number of miscellaneous components (0). The network ID is used in the description of energy hubs’ inputs and outputs, as discussed in Section 3.2. Network type specifies the expected format used to represent the physical constraint parameters. The number of miscellaneous components provides a way to describe network-specific components, such as natural gas compressor stations. Since no such components are needed to describe the electrical network, its value is 0 in the example.

The next four lines are necessary to construct the node-arc-incidence matrix, and follow the same format for each arc. For example, Line 2 in Listing 2 states that node 1 and node 2 are connected with a parameter-value ( $x_{ij}$ ) of 0.05 p.u. reactance, and a per unit flow capacity of 10.

After describing each arc of the network, we can determine  $\mathbf{A}$ , but we still need to determine  $\mathbf{G}_A$  and  $\mathbf{D}_A$  to fully represent the network. To accomplish this, we state which nodes are generators and loads (1 and 3, respectively). In addition, our format allows the user to specify per unit limits on generation  $\text{lim}(0, 100)$  and loads (fixed at 1 in example), as well as associated linear and quadratic costs for use in the objective function, (9, 0.09). Furthermore, the limits on generators and loads do not have to be numeric. In fact, an expression with variable generator or load limits is permitted by our format. For example, to denote a variable upper bound on the electric generator replace  $\text{lim}(0, 100)$

with  $\text{lim}(0, P_{g\_el})$ , where  $P_{g\_el}$  is a variable (vector) pre-defined in MATLAB. The format for other types of networks is similar, but with different network-specific arc parameters.

#### 4 Simulation

The format described in Section 3 allows the construction of arbitrarily large interconnected energy hub networks and, together with MATLAB and CPLEX, seamlessly allows solution of optimal power dispatch problems formulated in (37a)-(37y).

##### 4.1 System Construction

Our example energy hub system consists of an electrical network, a natural gas network, district heat loads, and wind generators. Energy hubs couple the four different energy types. To construct a large energy hub network, we employed the technique proposed in [11] for building random grids. That technique assumes uniform node location, exponential expected link length distribution, and poisson distribution for arc selection. Due to the size and random construction of the electrical and natural gas networks, a meaningful visualization of the energy hub system is not straightforward and is excluded here. However, via modification of graph drawing software, such as Tulip [12], visualization is a possibility for the future.

Network	$\langle k \rangle$	$N$	$E$	$G$	$D$
Electrical	4.36	100	218	12	22
Gas	4.88	100	244	8	8
Wind	0	20	0	20	0
Heat	0	30	0	0	30

Table 2: Topological characteristics of energy networks.

The topological characteristics of our system are given in Table 2. The values  $N$ ,  $E$ ,  $G$ , and  $D$  represent the number of nodes, arcs, generators, and loads, respectively, while  $\langle k \rangle$  is the average nodal degree. The wind and heat networks have no arcs and consist of generators and demands, respectively. We employed 102 energy hubs to couple the four networks via randomly selected nodes. The energy hubs are used to connect from the electrical network to gas and heat networks, from the gas network to electrical and heat networks, and from the wind network to the electrical network. All other network couplings, i.e. from gas to wind, are excluded in this simulation. All hubs connecting the wind network to the electrical network have output storage, while hub storage is added randomly to 75% of the remaining hubs. The system is assigned 24 time-intervals, corresponding to one complete day of operation. The consumer demand (load) and generation costs are set to peak near midday, while wind power is available mostly in the early and later parts of the day.

##### 4.2 Simulation Results

The large hub system of Table 2 was represented using the ASCII format of Section 3, which allowed di-

rect construction of all the matrices necessary for solving the optimal dispatch problem (37). The formulation employed quadratic generator costs, resulting in a multi-period mixed-integer quadratic programming problem with 1942 (118 integer) variables per one-hour time-step. The problem was solved in 253 seconds inside MATLAB with CPLEX on a 2.8 GHz Intel Core 2 Duo MacBook Pro with 4 GB RAM. The results are shown in Figures 5 and 6.

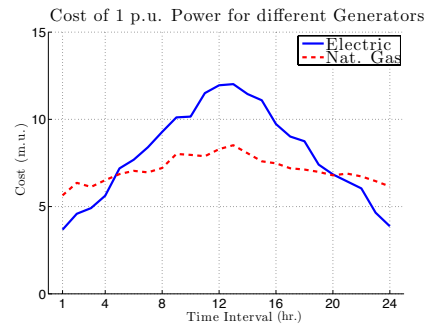


Figure 4: Example of generator costs over the 24-hour period.

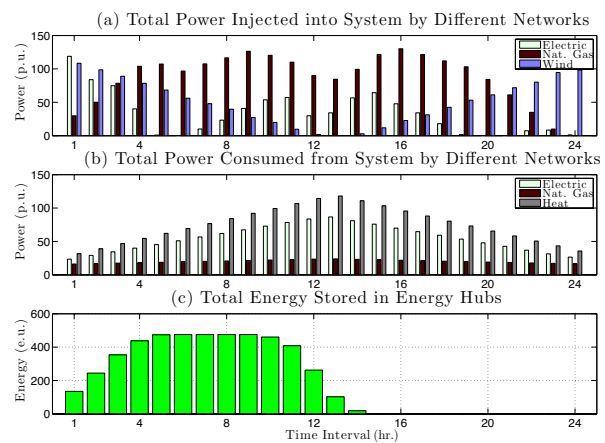


Figure 5: Results of optimal power dispatch over 24-hour period.

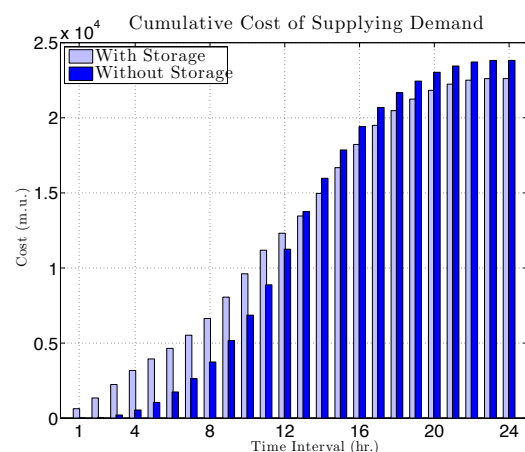


Figure 6: Cumulative cost comparison for energy hub systems with and without storage over 24-hour period.

We assume the cost of wind power generation is zero. In Figure 4, the costs of electrical energy and natural gas, given in monetary units (m.u.), vary with time, peaking at around interval 12-13. Consumer demand peaks at that time, as depicted in Figure 5(b), raising the cost of supply.

To minimize overall generator dispatch costs, we see in Figure 5(a) that the electrical and wind generators initially inject a large amount of relatively cheap power into the system. This surplus injected power is utilized by energy hub storage devices as depicted in Figure 5(c) to maximize storage *before* the generator costs and consumer demand reach their respective peaks near time-interval 13. After building up the energy storage levels, the available wind power decreases during the middle of the day. Storage is utilized during the peak period to minimize generation during the most costly intervals. After time interval 18, the wind is strong enough to supply all electrical loads and most of the gas and heating loads.

The impact of storage on the total cost over the 24 time intervals is shown Figure 6. Building up the energy storage levels incurs a non-trivial initial cost. However, due to the time-varying price of generation, an overall savings of 5% is achieved when compared to the same system with no storage. In fact, as depicted in Figure 6, the system with no storage becomes more expensive to operate at time-interval 13, which coincides with peak consumer demand. The ability to store low-cost energy and inject it during more expensive periods provides overall savings.

It is worth keeping in mind that these studies were performed on a non-trivial hub network that included 250 nodes and 102 hubs.

## 5 Conclusions and Extensions

This paper presents a novel method for describing general multi-carrier energy hub systems. This was accomplished by decomposing the energy hub formulation using dispatch factors and a binary expansion of the storage charge and discharge flows. With this format, we can take advantage of the flexible nature of energy hub models, and easily construct or alter large energy-hub networks.

Further investigations will improve upon the random grid generator to generalize construction of random energy hubs for linking between networks. Taking into account the entire horizon in the multi-period formulation leads to very large optimization problems. Therefore, we are interested in applying integer programming techniques to allow larger networks to be solved more efficiently.

Finally, we are interested in extending this work to include the study of large-scale cascading failures, which have been studied extensively in decoupled electrical networks [13, 14, 15]. However, research on cascading failures in large multi-energy systems has generally not considered the concept of energy hubs [16]. Simulating cascading failures requires large networks and these tools will allow us to establish and manipulate large energy-hub systems in an efficient manner.

## 6 Acknowledgments

We would like to thank the U.S. Department of Energy for funding under research grant DE-SC0002283 and Professor Amy Cohn for her valuable advice.

## REFERENCES

- [1] U.S.-Canada Power System Outage Task Force, "Final report on the august 14, 2003 Blackout in the united states and canada: Causes and recommendations," 2004.
- [2] A. Wood and B. Wollenberg, *Power Generation, Operation, and Control*. Wiley-Interscience, second ed., 1996.
- [3] M. Geidl, G. Koeppel, P. Favre-Perrod, B. Klockl, G. Andersson, and K. Frohlich, "Energy hubs for the future," *Power and Energy Magazine, IEEE*, vol. 5, no. 1, pp. 24–30, 2007.
- [4] H. Groscurth, T. Bruckner, and R. Kümmel, "Modeling of energy-services supply systems," *Energy*, vol. 20, no. 9, pp. 941–958, 1995.
- [5] S. Rinaldi, J. P. Peerenboom, and T. K. Kelly, "Identifying, understanding, and analyzing critical infrastructure interdependencies," *Control Systems Magazine, IEEE*, vol. 21, no. 6, pp. 11–25, 2001.
- [6] B. Bakken, H. Skjelbred, and O. Wolfgang, "etransport: Investment planning in energy supply systems with multiple energy carriers," *Energy*, vol. 32, pp. 1676–1689, 2007.
- [7] M. Geidl and G. Andersson, "A modeling and optimization approach for multiple energy carrier power flow," *In Proc. of IEEE PES PowerTech, St. Petersburg, Russian Federation*, pp. 1–7, 2005.
- [8] A. del Real, M. Galus, C. Bordons, and G. Andersson, "Optimal power dispatch of energy networks including external power exchange," *European Control Conference 2009 in Budapest, Hungary*, vol. 9, 2009.
- [9] M. Geidl and G. Andersson, "Optimal coupling of energy infrastructures," *IEEE Power Tech Lausanne*, pp. 1398–1403, 2007.
- [10] A. Osiadacz, *Simulation and Analysis of Gas Networks*. Gulf, first ed., 1987.
- [11] Z. Wang, R. Thomas, and A. Scaglione, "Generating random topology power grids," *Proceedings of the 41st Hawaii International Conference on System Sciences*, pp. 1–9, 2008.
- [12] D. Auber and F. Jourdan, "Interactive refinement of multi-scale network clusterings," *Proceedings of Ninth International Conference on Information Visualisation*, pp. 703–709, 2005.
- [13] D. Bienstock and A. Verma, "The N-k problem in power grids: New models, formulations, and numerical experiments," *SIAM Journal on Optimization*, vol. 20, no. 5, pp. 2352–2380, 2010.
- [14] H. Ren and I. Dobson, "Using transmission line outage data to estimate cascading failure propagation in an electric power system," *Circuits and Systems II: Express Briefs, IEEE Transactions on*, vol. 55, no. 9, pp. 927–931, 2008.
- [15] A. Pinar, J. Meza, V. Donde, and B. Lesieutre, "Optimization strategies for the vulnerability analysis of the electric power grid," *SIAM Journal on Optimization*, vol. 20, no. 4, pp. 1786–1810, 2010.
- [16] S. Buldyrev, R. Parshani, G. Paul, H. Stanley, and S. Havlin, "Catastrophic cascade of failures in interdependent networks," *Nature*, vol. 464, no. 7291, pp. 1025–1028, 2010.